THE AMERICAN SOCIETY OF MECHANICAL ENGINEERS
345 E. 47th St., New York, N.Y. 10017

94-GT-322

STALL INCEPTION IN A HIGH-SPEED LOW ASPECT RATIO FAN INCLUDING THE EFFECTS OF CASING TREATMENTS

S. E. Gorrell
Wright Laboratory
Wright-Patterson AFB, Ohio

P. M. Russler
Battelle Memorial Institute
Dayton, Ohio

ABSTRACT

The stall inception process in high-speed compressor components is important to understand in order to increase stage loading while maintaining stall margin. This paper presents the results of an in depth experimental investigation on the stall inception of a two stage, high-speed, low aspect ratio fan that is representative of current operational commercial and military fan technology. High-response static pressure measurements are presented which detail the stall inception process of the fan under various operating conditions. These conditions include: varied corrected speeds, a smooth case, a circumferential groove casing treatment, and a recirculating cavity casing treatment. Stage pressure characteristics and radial pressure ratio profiles are presented for the different operating conditions. The stage performance data, together with the static pressure data, are analyzed to provide a clear and thorough understanding of the stall inception process and how the process may vary under different conditions. Experimental results show that a stage may stall on the positive, neutral, or negative sloped part of the pressure characteristic. The three casing treatments had a significant effect on the rotor tip flow and these variations changed the stall inception path of the fan. Stall inception was characterized by the formation of a stall inception cell which grew to fully developed rotating stall. Properties affected by the changing tip flow include the stall inception duration, stall inception cell frequency, existence of modal waves, duration of modal waves, and modal wave frequency. In some instances modal waves appear to play a role in stall inception, in others they do not.

INTRODUCTION

The current trend in compressor design technology as it relates to the aircraft gas turbine engine is to obtain a high pressure ratio per stage. High stage loading reduces the number of compressor stages resulting in increased thrust to weight ratio for the engine. The operating region of a compressor is bounded on the high flow end by blade passage choking and on the low flow end by blade and/or endwall stalling. When the flow rate for a compressor drops below the stall line, two types of flow instability may occur: surge and/or rotating stall. Both surge and rotating stall are undesirable from the standpoint of engine operation and engine fatigue. These instabilities result in a reduced flow rate and pressure rise, a drop in efficiency, low engine thrust, elevated turbine temperatures, and high blade stress levels.

For most high speed compressors the design operating point is not normally near its highest pressure ratio as this tends to be close to the stall line (Fig. 1). When operating near the stall line, inlet distortion or other flow instabilities may drive the compressor to rotating stall or surge. For this reason a

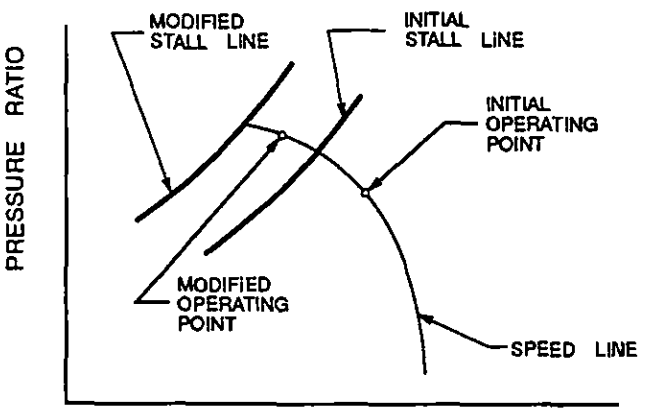

Figure 1. Extending Compressor Operating Range

Presented at the International Gas Turbine and Aeroengine Congress and Exposition
The Hague, Netherlands — June 13–16, 1994

compressor is designed to operate with a stall margin. Stall margin is the measure of the operating range between the compressor operating point and the onset of system instability (the stall line). If the stall line is moved to a lower mass flow and/or higher pressure ratio as shown in Fig. 1, the compressor may operate at a higher pressure ratio while maintaining its desired stall margin. Passive and active control are two methods that have been investigated to accomplish this. Casing treatments were shown by Prince et al (1975) and Takata and Tsukuda (1975) to be an effective means of decreasing the mass flow rate at which stall occurs, thus increasing stall margin. More recently it has been proposed by Epstein et al (1986) that stall margin may be increased by actively controlling and delaying the onset of stall. Day (1993a) and Paduano et al (1991) successfully demonstrated this by applying active control to introduce flow perturbations which damped the disturbances leading to stall inception.

A better understanding of stall inception will greatly increase the ability to apply casing treatments and active control technology. Greitzer et al (1979) showed that casing treatments were most effective when compressor stall initiated at the casing wall. Smith and Cumpsty (1984) added that successful casing treatments provide a flow path between the blade pressure and suction surfaces so a small portion of the flow can be recirculated. However, Smith and Cumpsty stated that why casing treatments are effective could not be completely understood until the flow mechanism leading to stall is understood. Furthermore, in order to control a compressor as it approaches stall it has become important to clearly understand when and how the stall inception process takes place. A clear understanding of stall inception in high speed compressors will improve the understanding of the role of tip clearance, casing treatments, and active control on compressor stability.

The purpose of this paper is to present for the first time data from a high speed, highly loaded, low aspect ratio fan. Data will also be presented for the first time on the effects of casing treatments on stall inception. This will result in a better understanding of the stall inception process as it applies to the use of casing treatments and active control to extend the stall margin and allow for higher stage loading. This will be accomplished with a thorough steady-state and transient analysis of the compressor. Steady-state data will show the pressure characteristic shape and radial pressure profile of the compressor with different casing treatments. High-response static pressure measurements will detail the stall inception process. It will then be possible to understand how the near-stall operating conditions of the compressor relate to stall inception.

STALL INCEPTION

Recent experiments conducted by Day (1993b) support two models to describe the stall inception process. The classical description given by Emmons (1955) is that stall inception is caused by separation of flow on the blade due to changes in incidence caused by some disturbance in the flow field. This model of stall inception has been demonstrated in low speed machines by Day (1993b) and in high speed machines by Day and Freeman (1993). Their results showed that the stall cell at inception only affected a few blade rows and that the frequency of the stall cell at inception was significantly higher than the frequency of the fully developed stall cell.

The second stall inception model was proposed by Moore and Greitzer (1986) and is based on modal analysis. Small amplitude sinusoidal modal (or rotating) waves of circumferential length scale appear prior to stall and rotate around the circumference of the compressor annulus. As the stage is throttled toward stall, the rotating waves grow smoothly until a fully developed rotating stall cell is formed. In theory the frequency of the modal wave and the fully developed rotating stall cell should be the same. These disturbances have been shown to exist in low speed compressors by McDougall et al (1990), Garnier et al (1991), and Day (1993a & b). Recently, rotating waves have been observed in high speed compressors as reported by Garnier et al (1991), Boyer and King (1993), and Hoying (1993). However, these high speed experiments focused on determining the existence of rotating waves prior to stall, not if it were the rotating waves themselves which grew into fully developed rotating stall.

TEST COMPRESSOR

The test compressor is a high-speed, two stage, low aspect ratio fan as shown in Fig. 2. Airfoil geometry parameters are given in Table 1. Rotor 1 is transonic with an inlet relative Mach number greater than one over the outer 80% span. The tip relative Mach number is 1.69 at the aerodynamic design point. Stator 1 is a tandem vane configuration made up of a stationary strut and variable flap. The baseline configuration of the fan with a circumferential groove casing treatment over rotor 1 had been tested previously. The demonstrated performance at design conditions are shown in Table 2.

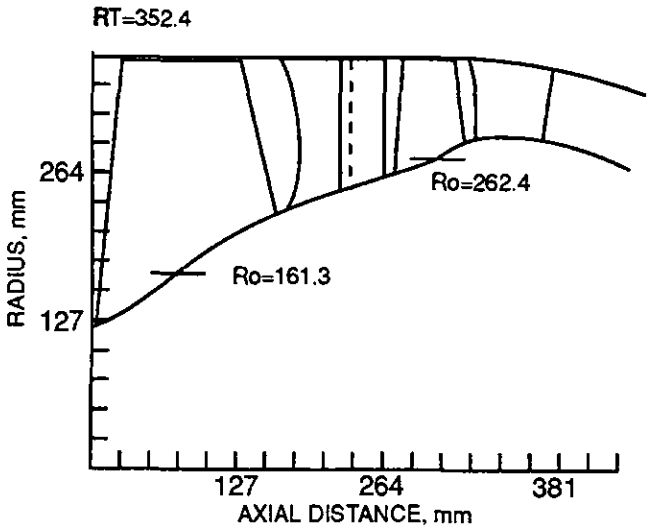

Figure 2. Meridional View of Test Compressor

Table 1. Airfoil Geometry Parameters

Airfoil	Number of Blades	Radius Ratio		Aspect Ratio	Solidity		Tm/c	
		Inlet	Avg	Root	ID	OD	ID	OD
R1	16	0.33	0.47	1.10	2.67	1.50	0.087	0.028
S1S	41	0.63	0.65	2.36	1.45	1.30	0.057	0.087
S1F	41	0.67	0.69	2.90	1.06	0.72	0.050	0.080
R2	40	0.72	0.75	1.09	1.95	1.47	0.080	0.030
S2	60	0.80	0.81	1.16	1.93	1.90	0.056	0.090

Table 2. Baseline Fan Performance at Design

Parameter	Demonstrated Value
Corrected Speed, RPM	13022
Total Pressure Ratio	4.30
Corrected Tip Speed, m/s	480.67
Corrected Mass Flow, kg/s	71.80
Flow/Annulus Area,kg/s/m^2	206.53
Adiabatic Efficiency	0.852
Stall Margin, %	13

Three different casings were tested over rotor 1: smooth case, circumferential groove, and a recirculating cavity treatment. Casing treatment geometry is detailed in Table 3 and Fig. 3. The recirculating cavity casing treatment is a combination of an axial skewed slot with a recirculation area above the slots. The recirculating area is 80.0 mm long and 17.8 mm deep. The recirculating cavity covers all slots which allows the slots to communicate with each other. The cold tip clearance for all three casing treatments was 0.89% of tip chord.

Table 3. Casing Treatment Geometry

Geometry	Circ Grooves	Recirc Cavity
Axial Length/Projected Tip Axial Chord	0.53	0.41
Width (mm)	8.6	5.6
Depth (mm)	26.7	10.2
Spacing (mm)	4.3	9.7
Axial Slot Angle (deg)	—	15
Radial Slot Angle (deg)	—	50

DATA ACQUISITION AND REDUCTION

The fan was tested at the Compressor Research Facility (CRF), Wright Laboratory, located at Wright-Patterson Air Force Base. The CRF is one of the two high-speed test facilities at Wright Laboratory and was described by Ostdiek et al (1989).

Data used to define the steady-state performance of the compressor were acquired with the digital data system. Data were obtained by calculating the average of 30 samples taken over a time period of 195 ms. The radial profile and pressure characteristic plots presented in this paper used the steady-state data acquired by the digital data system.

High-response pressure data were obtained from sixteen high frequency response transducers measuring static pressure through taps in the outer case. Eight taps located approximately 45 degrees apart along the circumference allowed static pressure at the leading edge of each of the two rotors to be recorded.

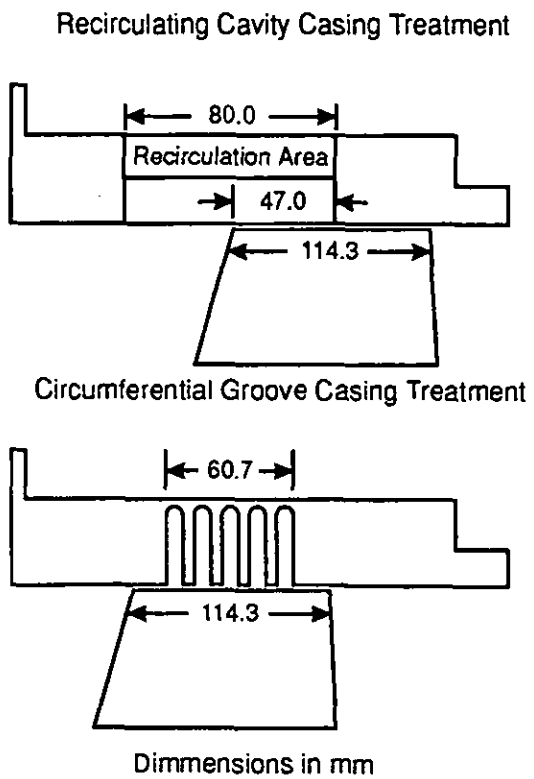

Figure 3. Casing Treatments

Pressure fluctuations with frequencies of less than 1 kHz could be monitored and recorded on analog tape with this configuration. The analog signals were then low-pass filtered with an analog filter to avoid aliasing during the digitizing process. The transducer signals were digitally sampled at 5000 samples-per-second, allowing the resolution of frequencies up to the 1 kHz frequency response limit of the instrumentation. The digitized data sets were then high pass filtered with a digital Finite Impulse Response (FIR) filter to remove DC offset. The high-response static pressure plots presented in the paper used this data.

A preliminary review of the digitized data suggested that any pre-stall rotating waves would have small amplitudes compared to the rotor frequency and/or any electrical background noise. Therefore, it was necessary to create another set of filtered data before further signal processing could be accomplished. Noise reduction and removal of rotor frequency was accomplished by band pass filtering the digitized data in lattice form with Infinite Impulse Response (IIR) filters as presented by Stearns and David (1993). This type of filtering provided sharp frequency cut-off and minimized the phase shift in the data.

Although the actual rotating wave is not likely to be a perfect sinusoid, the mode with the greatest amplitude (or magnitude) will tend to dominate the character of the rotating wave. An attempt was made to find such waves in the data presented in this paper by using a Spatial Fourier Transform (SFT) algorithm. This algorithm, in its simplest form, is based on the following equation:

$$C_k = \frac{1}{N}\sum_{n=1}^{N} x_n e^{\left(\frac{-2ikn\pi}{N}\right)} \qquad (1)$$

where x_n represents the individual pressure measurements at a given time, N is the number of individual measurements, and k is the mode number. Because there are eight static pressure traces per stage in this study, N=8. Eight measurement locations allowed the first three modes to be resolved. Since the taps in the compressor case were not exactly 45 degrees apart, and therefore not equally spaced, a modified form of equation 1 was used. This modified equation is described in Garnier et al (1991).

Marching in time, the algorithm applied the equation at each time step in the data. The complex Fourier coefficients that result were converted into magnitude and phase information. This allowed the magnitude and phase of each of the three modes to be plotted against time.

EXPERIMENTAL RESULTS

This data was analyzed from the standpoint of its relationship to stall inception. A detailed investigation into the performance of the different casing treatments will be the subject of another paper.

Overall and Stage Performance

Figure 4 shows the overall pressure ratio and efficiency versus corrected mass flow for the test compressor. Design flow and pressure ratio were obtained at 98.6% design corrected speed. At 98.6% speed it is observed that the recirculating cavity casing treatment did not demonstrate similar performance to the other casings. It operated at a lower mass flow, pressure ratio, and efficiency than the smooth case and circumferential groove casing treatment. At 85% all three casings operate at similar mass flow, pressure ratio, and efficiency. The 68% plots show an increased pressure ratio for the recirculating cavity casing treatment. The smooth case and circumferential groove casing treatment are almost identical.

The slope of the pressure characteristic was determined from a review of data recorded at 5 Hz as the fan was throttled to stall. The smooth case pressure characteristic at stall was neutrally sloped at 98.6%, and positively sloped at 85% and 68%. For all speeds the circumferential groove and recirculating cavity casing treatment pressure characteristics were positively sloped at stall. The corrected mass flow at stall was always lowest for the recirculating cavity, followed by circumferential groove, and finally the smooth case. Progressive stall was observed at 68% design corrected speed and abrupt stall at 85% and 98.6%.

Table 4 compares the mass flow for each steady-state near-stall operating point with that of the smooth case. For the recirculating cavity casing treatment at 98.6% speed the percent change from the smooth case is a result of performance drop, not stall margin increase.

A plot of pressure ratio versus corrected mass flow for rotor 1 is provided in Fig. 5. The smooth case pressure characteristic shape at stall was slightly negatively sloped at 98.6% speed, neutrally sloped at 85% speed, and positively sloped at 68% speed. The circumferential groove casing treatment was positively sloped at 98.6% and 68% design corrected speed, and

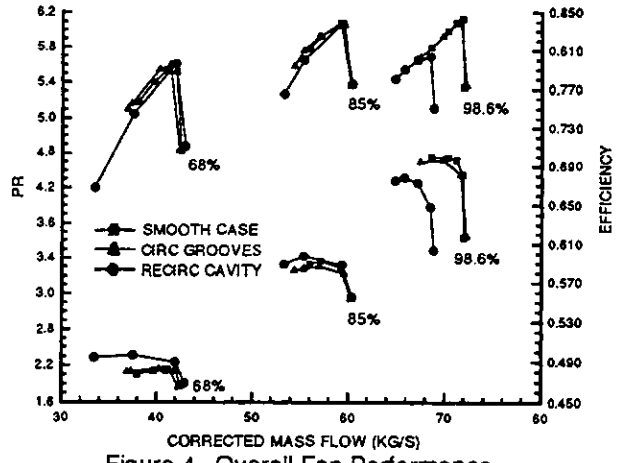

Figure 4. Overall Fan Performance

Table 4. Steady-State Near-Stall Mass Flow

Casing Treatment	Mass Flow at Near-Stall (kg/s)			% Change From Smooth Case		
	98.6%	85%	68%	98.6%	85%	68%
Smooth Case	68.54	55.96	37.99	—	—	—
Circumferential Groove	67.41	54.32	36.89	1.649	2.931	2.90
Recirculating Cavity	64.37	53.27	33.46	6.084	4.807	11.92

neutrally sloped at 85%. The recirculating cavity casing treatment was positively sloped at 98.6%, neutrally sloped at 85%, and negatively sloped at 68% speed. The reduced performance at 98.6% speed for recirculating cavity is probably a result of blockage induced by the recirculating flow which restricted the amount of total flow the rotor was able to pass.

The stator 1-rotor 2 pressure characteristics are shown in Fig. 6. With the exception of the recirculating cavity casing treatment at 98.6% design corrected speed, the stage operated on the same characteristic for all three casings. At 98.6% speed, the recirculating cavity characteristic was down in mass flow because of the reduced flow being passed by rotor 1. With the exception just noted, the effect of the different casing treatments was to lower the mass flow at stall on the characteristic. In all cases, as the second stage approached stall the shape of all the pressure characteristics were positive.

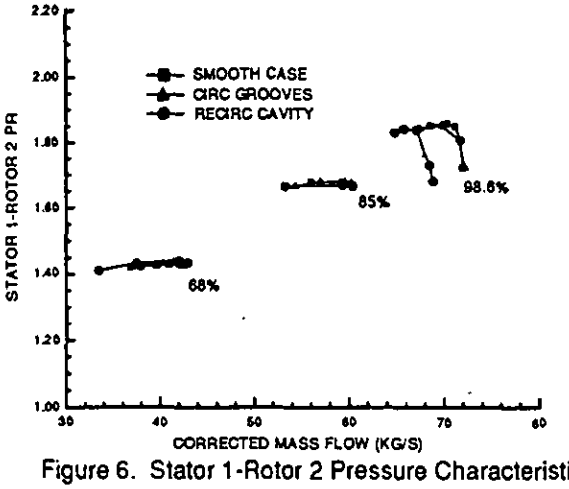

Figure 6. Stator 1-Rotor 2 Pressure Characteristic

Stage Matching

From looking at the overall, rotor 1, and stator 1-rotor 2 pressure characteristics (Figs. 4-6) it is observed that the fan is very well matched at all three speeds. When the fan operates near stall both stages are at their near stall points also. These observations were true for all three casing treatments.

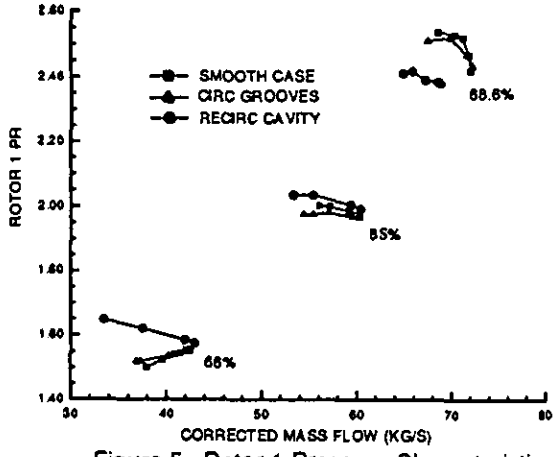

Figure 5. Rotor 1 Pressure Characteristic

Radial Pressure Ratio Profiles

The data from the radial pressure ratio profiles were analyzed to help understand what effect the casing treatments had on blade loading as the fan approached stall. The pressure ratio was determined from total pressure rakes located upstream of the rotor and stator 1 leading edge vane mounted total pressure probes. The pressure ratio profiles were examined by observing the magnitude and shape of the profiles and how they changed with the various casing treatments.

Figures 7 through 9 show the radial pressure profiles for 68%, 85%, and 98.6% design corrected speed at the near-stall steady-state operating condition. Because of a mechanical failure of the recirculating cavity hardware, steady-state data were not obtained at the near stall condition at 98.6% speed. At 68% speed (Fig. 7) there is a slight deficiency in the hub element for all casing treatments. This is most likely a result of corner separation. The profiles for the smooth and circumferential groove casing treatment are very similar in shape. The profile continually weakens from the hub to 70% span then increases in strength from 70% span to the tip. The magnitude of the circumferential groove casing treatment is higher than the smooth case. The recirculating cavity casing treatment has a nearly constant profile from the hub to 70% span and then increases in strength toward the tip. Following the trends seen from the rotor 1 pressure characteristic data (Fig. 5), the profile magnitude at the near-stall condition is

greatest for the recirculating cavity, followed by the circumferential grooves and smooth case.

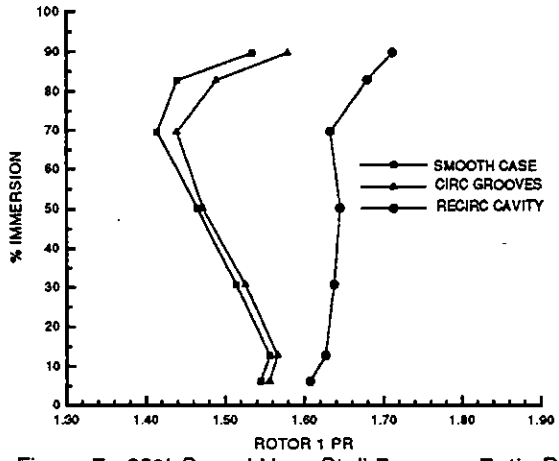

Figure 7. 68% Speed Near-Stall Pressure Ratio Profile

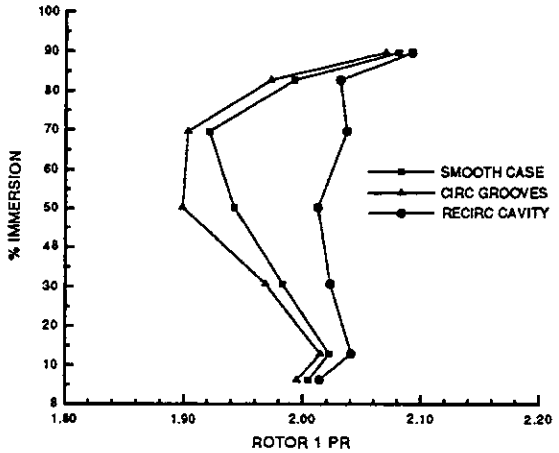

Figure 8. 85% Speed Near-Stall Pressure Ratio Profile

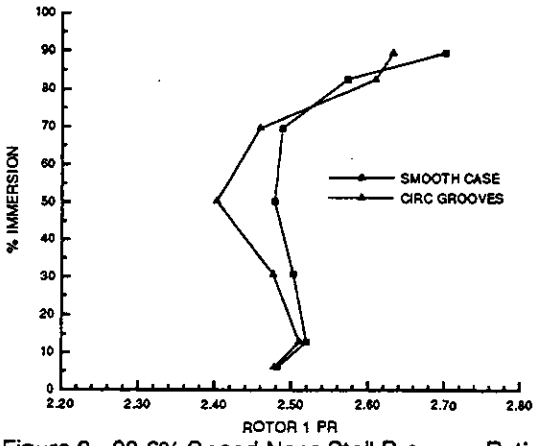

Figure 9. 98.6% Speed Near-Stall Pressure Ratio Profile

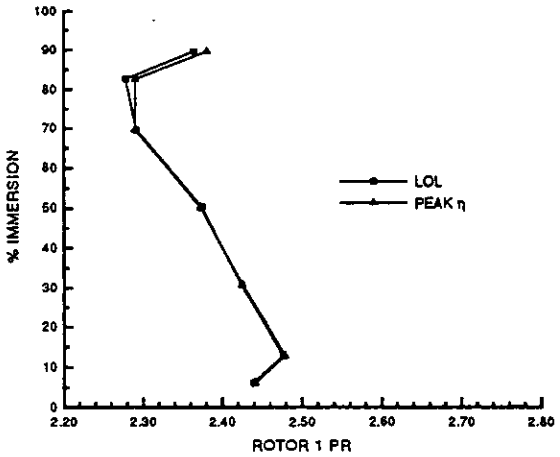

Figure 10. 98.6% Speed Recirc Cavity Pressure Ratio Profile

At 85% speed (Fig. 8) the hub corner separation is present for all casing treatments. The smooth case and circumferential groove casing treatments are both strong at the hub and tip while weak at the mid span (30% to 80% span). The recirculating cavity casing treatment has a nearly constant profile from 10% to 80% span and then strengthens at the tip. In terms of loading magnitude, the profiles follow what was seen in the pressure characteristic data. The recirculating cavity had the highest pressure ratio near stall, followed by the smooth case and circumferential groove.

The radial pressure ratio profiles at 98.6% design corrected speed (Fig. 9) show a hub corner separation similar to that seen at 68% and 85% speed. The circumferential groove casing treatment was strong at the hub and tip but still weak at the mid span. The profile did weaken slightly at the tip element. The smooth case had a nearly constant profile from 10% to 70% span and then increased in strength to the tip. It was difficult to predict what the recirculating cavity casing treatment profile would have looked like at this speed. Figure 10 shows the radial pressure ratio profile for this casing treatment for the low operating line (LOL) and peak efficiency conditions. Since the rotor 1 pressure characteristic (see Fig. 5) varied little in magnitude from the LOL to near-stall condition, it is possible that a near-stall profile would be similar to the LOL and peak efficiency profiles from the hub to 70% span and then increase in magnitude while maintaining a similar shape from 70% span to the tip.

High-Response Static Pressures

The high-response static pressure measurements gave a very clear and accurate picture of the stall inception process. The data presented in Figs. 11 through 17 are low and high pass filtered only. At 68% design corrected speed (Fig. 14) the fan exhibited progressive stall. For all three casing treatments a stall cell formed at a mass flow greater than the near-stall operating point on the pressure characteristic and is most likely a part span (tip) stall cell. This behavior has been observed in

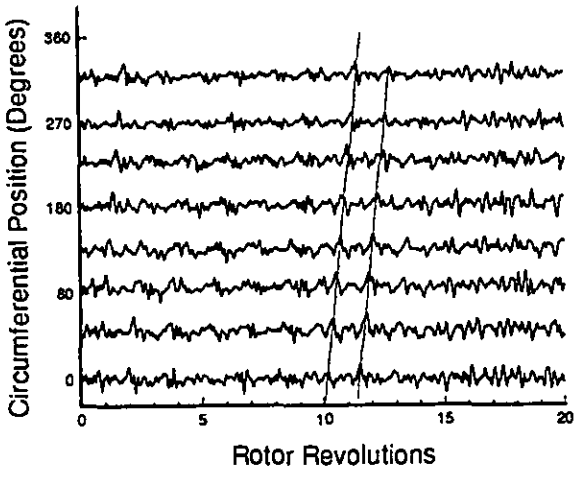

Figure 11. 68% Speed Pre-Stall Operating Point

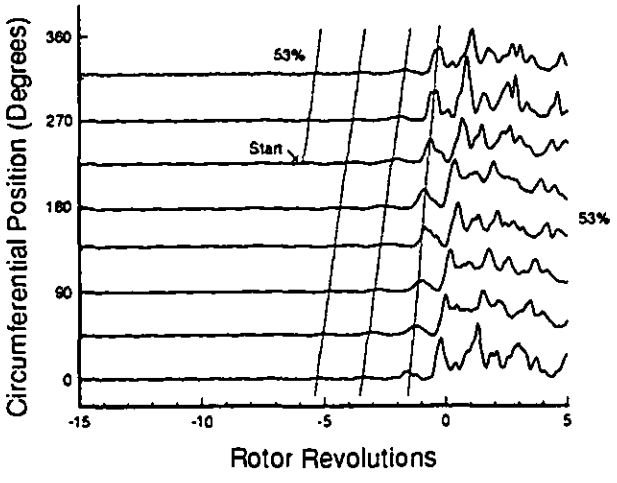

Figure 12. Stall Inception at 98.6% Speed Smooth Case

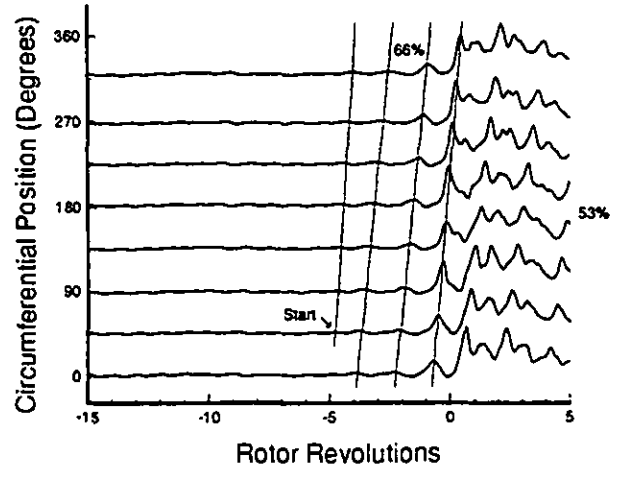

Figure 13. Stall Inception at 98.6% Speed Circ Grooves

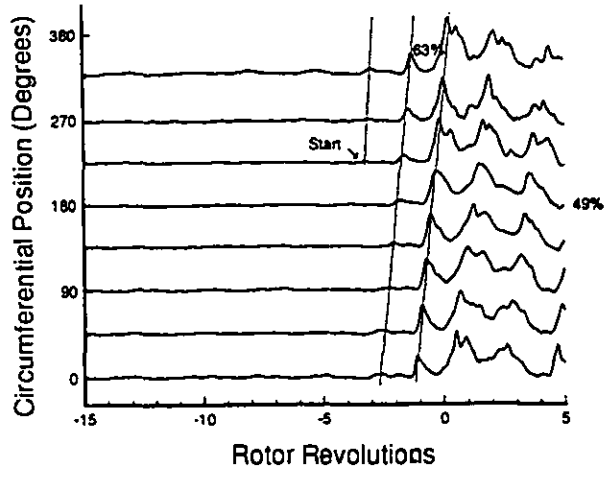

Figure 14. Stall Inception at 98.6% Speed Recirc Cavity

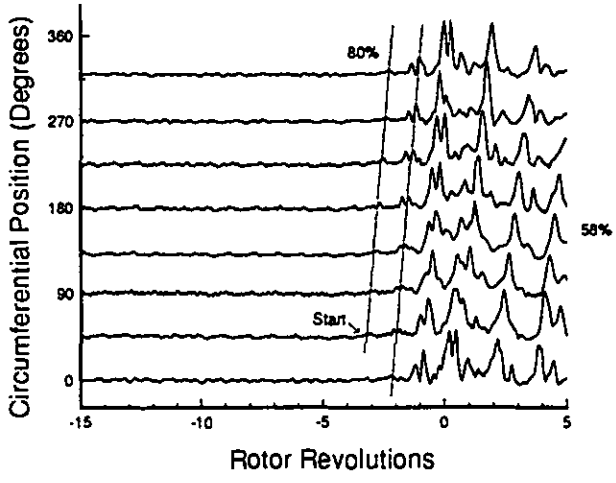

Figure 15. Stall Inception at 85% Speed Smooth Case

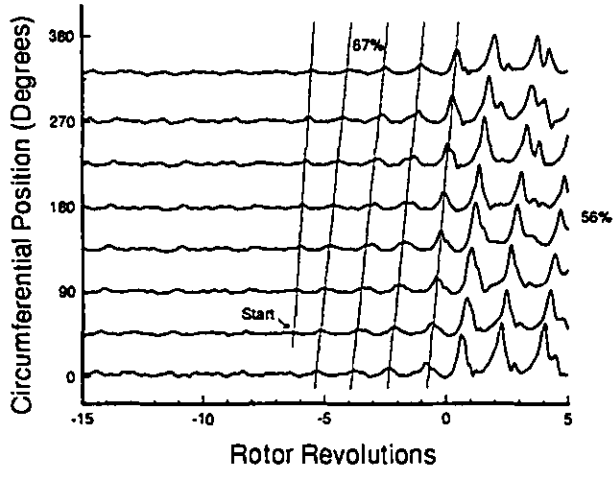

Figure 16. Stall Inception at 85% Speed Circ Grooves

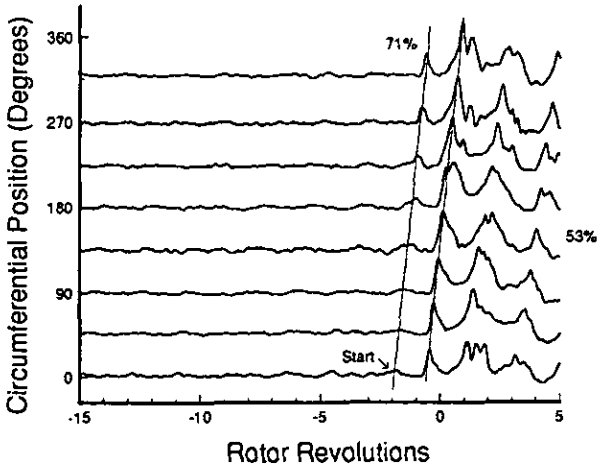

Figure 17. Stall Inception at 85% Speed Recirc Cavity

other compressors that demonstrate progressive stall. Because of the progressive nature of the stall at 68% speed, the stall inception process was not looked at in detail.

The high-response static pressure measurements from rotor 1 leading edge were the clearest and most informative to document stall inception in the fan. The rotor 2 leading edge measurements were similar to rotor 1 but also contained additional high frequency content as a result of the flow passing through rotor 1 and stator 1. The magnitude and frequency of the high-response pressure measurements can be analyzed to detail the stall inception process. When the fan has reached fully developed rotating stall the amplitude of the high-response static pressure traces fluctuates a large amount at a frequency less than the rotor speed. The speed of the fully developed rotating stall cell was determined from an FFT analysis of the in-stall data (a much longer scan than that shown in Figs. 12-17). Prior to stall the amplitudes of the high-response pressure measurements are significantly less than fully developed rotating stall. Stall inception is defined as an irreversible process during which a pressure oscillation with a frequency less than rotor speed increases in amplitude from pre-stall to fully developed rotating stall. This process is pointed out in Figs. 12-17 by solid lines. The frequency of the stall inception perturbation was determined from the figures.

Day (1993b) used the frequency of the signal in the stall inception region as a means to help distinguish whether modal waves or a finite stall cell caused the formation of fully developed rotating stall cell. A small stall cell rotating fast and slowing as it grows to fully developed rotating stall was interpreted as representative of the Emmons (1955) theory of stall inception. A stall cell growing progressively out of a modal wave with no abrupt change in speed between the modal wave and emerging stall cell was interpreted as representative of the Moore and Greitzer (1986) stall inception theory. The frequency of the stall inception data presented here was also useful in interpreting the results of this experiment.

Figures 12 through 14 show the stall inception process for the three different casings at 98.6% design corrected speed. Prior to stall, the rotor frequency signal is clearly evident and is dominant for the smooth case and circumferential groove casing treatment. Stall inception is characterized by an increase in static pressure magnitude at less than rotor frequency as a fully developed rotating stall cell forms. The rotor frequency signal is not clear for the recirculating cavity casing treatment prior to stall. However, the stall inception process itself is the same as the smooth case and circumferential groove casing treatment with the formation of a fully developed rotating stall cell in 4 rotor revolutions. Table 5 provides values for stall inception duration (rotor revolutions), stall inception frequency (percent rotor speed), and fully developed rotating stall frequency (percent rotor speed) for each speed and casing treatment.

Figures 15 through 17 show the stall inception process at 85% design corrected speed. Once again stall inception is characterized by an increase in amplitude at a speed less than rotor frequency which grows to fully developed rotating stall. The rotor frequency signal is evident in the smooth case but not as clear for the circumferential groove and recirculating cavity. The stall inception frequency is much greater than that observed

Table 5. Fan Stall Results

Speed (% Design)	98.6			85		
Casing Treatment	Smooth Case	Circ Grooves	Recirc Cavity	Smooth Case	Circ Grooves	Recirc Cavity
Stall Inception Duration (Revs)	6	5	4	3	6	2
Stall Inception Frequency (% Design)	53	66	63	80	67	71
Modal Wave Duration (Revs)	—	11	15,3	—	40	15,8
Modal Wave Frequency (% Design)	—	66	38,56	—	61	45,53
Fully Developed Rotating Stall Frequency (% Design)	53	53	49	58	56	53

at 98.6% speed. Stall inception was very short for the recirculating cavity making it difficult to determine the frequency of the stall cell at inception.

Trends from Table 5 show that stall inception occurs over a very short period of rotor revolutions, stall inception frequency is higher at 85% design corrected speed than 98.6% speed, and there is not much variation in the frequency of fully developed rotating stall for different casings. It is significant to note that for all stalls except 98.6% speed, smooth case, the frequency of the stall cell at inception was 11% to 22% faster than the fully developed rotating stall cell.

Modal Analysis

After analyzing the high-response static pressure data, the next step was to determine whether or not rotating waves were present and what role they played in the formation of a fully developed rotating stall cell. At 85% design corrected speed the recirculating cavity pre-stall data (Figs. 14 and 17) did appear to have a lower frequency signal present. The fact that the frequency of stall inception for the smooth case, 98.6% speed, is the same as the rotating stall frequency also suggested rotating waves could be present.

The high-response static pressure data were analyzed via Spatial Fourier Transform as described in the data acquisition section. This method was introduced and described by McDougall et al (1990) and Garnier et al (1991). In very simplified terms, if rotating waves exist then a constant slope of phase angle versus time would be present in one of the modes and the magnitude of the SFT would also increase. Using this method at 98.6% design corrected speed the smooth case shows no sign of rotating waves prior to stall inception. The circumferential groove and recirculating cavity do show a constant phase speed for the first mode prior to stall (Figs. 18 and 19). Table 5 presents values for modal wave duration prior to stall (rotor revolutions) and modal wave frequency (percent rotor speed) for each speed and casing combination. Close examination of the recirculating cavity phase data shows a change in slope corresponding to stall inception. The speed of the first mode is 38% rotor speed from -20 to -3 rotor revolutions and 56% rotor speed from -3 rotor revolutions to stall. The later is very close to the speed of the stall inception cell (63% rotor speed).

At 85% design corrected speed the smooth case again shows no sign of modal activity before stall inception. Figures 20 and 21 present the phase information for the circumferential groove and recirculating cavity casing treatments. The circumferential groove data shows the second mode phase angle at a constant slope of 190% rotor speed, very near the first harmonic of the rotor frequency. The recirculating cavity shows a constant phase speed of 45% rotor speed for -18 to -7.5 rotor revolution and 53% for the final 7.5 rotor revolutions to stall. The 53% is the same as the fully developed rotating stall frequency.

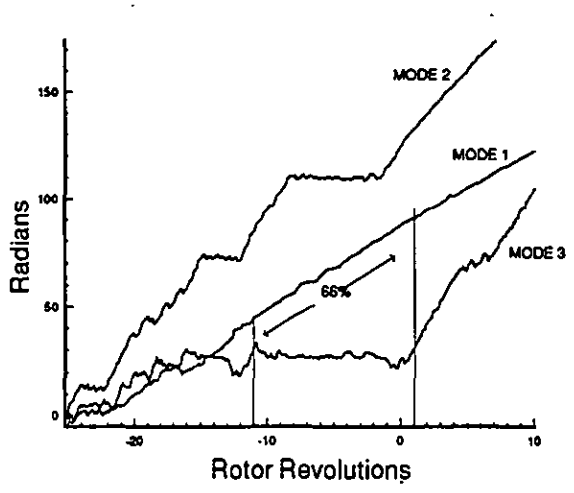

Figure 18. SFT Phase 98.6% Speed Circ Grooves

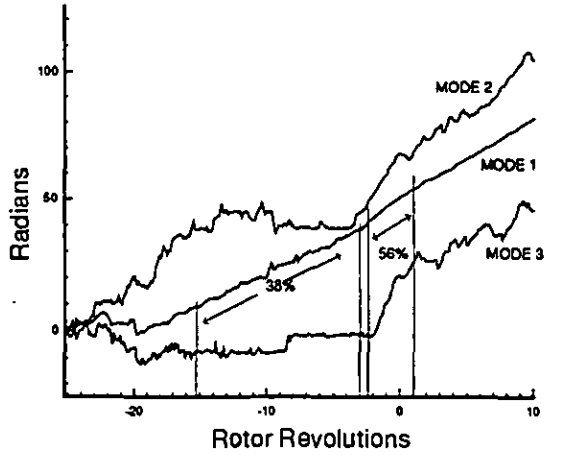

Figure 19. SFT Phase 98.6% Speed Recirc Cavity

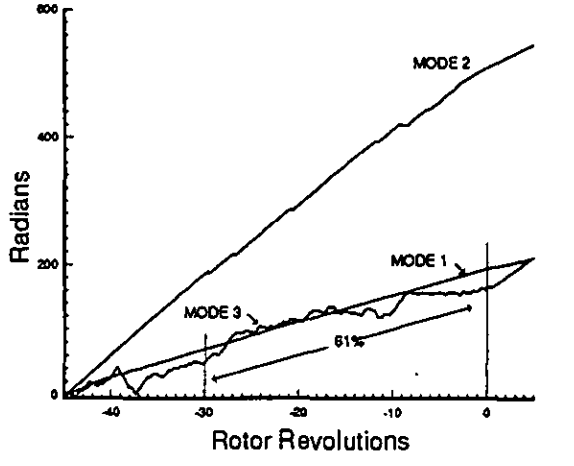

Figure 20. SFT Phase 85% Speed Circ Grooves

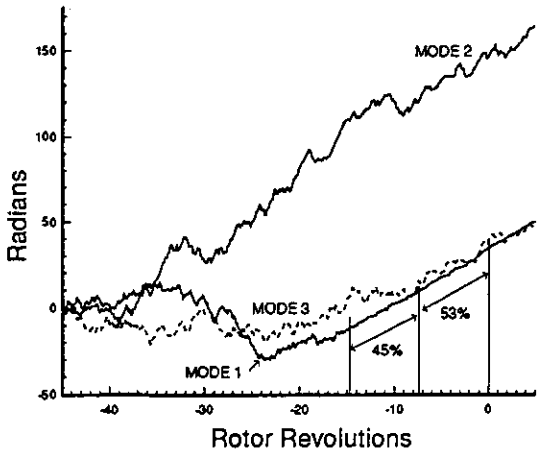

Figure 21. SFT Phase at 85% Speed Recirc Cavity

DISCUSSION

The casing treatments did have an impact on the shape of the pressure characteristic at stall. Circumferential grooves extended the range of the neutrally sloped portion of the characteristic at 85% speed and made the characteristic change from neutral to positively sloped at 68% and 98.6% speed. The recirculating cavity extended the neutrally sloped range at 85% speed and changed the characteristic from neutrally sloped to negatively sloped at 68% speed. Stall did not immediately follow once the peak of the characteristic was attained. There was often substantial flow range remaining after the peak was reached. The rotor 1 pressure characteristic data shows that stall inception could occur on a negative, neutral, or positive sloped characteristic. Overall characteristic shape was always neutral or positive at stall.

An observation made in some compressors is that the peak of the pressure characteristic is synonymous with the stage being very close to stall. Many models that are used to simulate compressor stability use the pressure characteristic peak as the stall point. The results of this paper suggest that for highly loaded transonic rotors the flow conditions favoring stall inception may happen on the negative, neutral, or positive slope of the stage characteristic. If conditions favoring stall occur at a higher mass flow, the characteristic may be negative or neutral sloped. If these conditions occur at a lower mass flow, the characteristic may be negative or positive sloped. For this fan the effect of the casing treatments was to inhibit the tip from stalling. This resulted in a lower mass flow at stall and thus a different characteristic shape. At the higher speeds the casing treatment changed the slope of the pressure characteristic near stall to positive. A possible explanation for this is that when the stage is operating near stall and the mass flow is reduced further, the casing treatments affect the tip flow so stall is delayed but at the same time losses in the tip increase which results in a lower pressure ratio, thus a positive sloped characteristic.

The smooth case and circumferential groove pressure ratio profiles show similar trends for 68%, 85%, and 98.6% design corrected speed. At 68% and 85% speed the recirculating cavity casing treatment allowed the rotor to be loaded higher in magnitude and nearly evenly loaded from hub to tip. The higher and more uniform loading corresponds to a higher pressure ratio and increased stall margin. However at 98.6% speed the recirculating cavity severely decreased the overall loading and mass flow through the rotor. There is a tradeoff between part speed and design performance for the recirculating cavity casing treatment. At part speed, the recirculation area is beneficial while at design speed it is degrading to performance. A useful experiment would be to optimize the recirculation area in such a casing treatment that will improve stall margin at part speed without sacrificing performance at design speed.

It is significant to note that for all stalls except 98.6% speed, smooth case, the frequency of the stall inception disturbance was 11% to 22% faster than the fully developed rotating stall cell. For both speeds, smooth case, no modal waves were detected. The authors are aware of a new method for detecting pre-stall waves (Tryfonidis et al 1994) using traveling wave energy. This concept is promising in that in many cases it provides more stall warning than the SFT phase method. However, since modal waves were observed for this fan with casing treatments, there is confidence that they can be detected when present. This research is concerned not with stall warning, but in understanding stall inception and what role modal waves play in that process. The authors therefore feel strongly that for this fan fully developed rotating stall grew from a stall inception cell. It may be that modal waves played a role in the formation of the stall inception cell and this will be discussed later in this section.

Each of the casing treatments produced a distinct flow pattern at the rotor tip at the near-stall operating point which in turn varied the stall inception characteristics of the fan. The high-response static pressure measurements show the rotor tip flow patterns and demonstrate how each casing treatment and speed combination had a unique stall inception path. Table 5 shows that for each speed, the fully developed rotating stall frequency changed only a little while the stall inception path varied greatly with each casing treatment. Casing treatments influenced the stall inception duration, stall inception cell frequency, existence of modal waves, duration of modal waves, and modal wave frequency.

Casing treatments may also alter the stall inception properties of a compressor in a similar manner as tip clearance. Casing treatments that increase the effective area over the rotor appear to show some similar trends as increasing the tip clearance. From the results presented here, rotating waves were apparent with casing treatments but not with the smooth case. This is interesting in light of an experiment presented by Day (1993b) where a compressor that did not initially exhibit modal waves showed them after the tip clearance was increased.

It is possible that the frequency of the stall inception cell is related to what circumferential extent of the rotor initially stalls at inception. If this is true, then at 98.6% speed many blades stalled at once (or nearly at once) which made for a larger and

slower stall inception cell. At 85% speed, less blades initially stalled and therefore the stall inception cell was smaller in circumferential size and faster in speed. If the different casing treatments affect the circumferential extent of the rotor that initially stalls, then even at a constant fan speed the stall inception cell speed may vary.

Modal waves were observed when casing treatments were installed. The challenge in understanding modal waves is determining if they are a precursor to stall or a product of the flow conditions which precede stall. In all instances when modal waves were detected, they were observed prior to the stall inception process defined by the high-response static pressure measurements. At 98.6% speed modal waves were observed from 6 to 11 rotor revolutions prior to stall inception and at 85% speed from 13 to 34 rotor revolutions.

Two types of modal activity are seen from the SFT phase information. One case observed from the 98.6% speed, circumferential groove casing treatment, is that modal waves are the same speed as the stall inception cell but significantly higher than the fully developed rotating stall frequency. This suggests that a stall inception cell grew from an established rotating wave of the same frequency. This observation could explain why the majority of high speed data referenced has shown modal wave frequencies higher than the fully developed rotating stall cell frequency. Remember that modal theory states the frequency of the modal waves and fully developed rotating stall cell should be the same. What may actually be seen in their SFT data are modal waves growing into a stall inception cell which is at a higher frequency than the fully developed rotating stall cell. A contrary interpretation is that a stall cell was present much earlier but was difficult to pick out from the high-response static pressure data.

The other case observed from the recirculating cavity casing treatment at 98.6% speed and both casing treatments at 85% speed, is that modal waves are slower than the stall inception cell. Also, for the recirculating cavity casing treatment at 85% and 98.6% speed, the modal wave speed changes (increases) as the stall inception process takes place. In these examples, a rotating wave below the fully developed rotating stall cell frequency is present but not strongly related to the stall inception cell. An example provided by Day (1993b) also showed a finite stall cell superimposed on a wave of much slower frequency. In these instances it is possible that modal waves are a response to the tip flow conditions that lead to stall inception. Interpretation of modal analysis results can be quite a challenge. It is difficult to distinguish between modal waves and a finite stall cell of large circumferential extent. Once a stall cell is formed the SFT will track it just as a modal wave. There is still much to learn to better understand what relationship modal waves have with the stall inception process.

CONCLUSIONS

Understanding the stall inception process in compressors can significantly help in advancing passive and active control technologies that seek to obtain a high pressure ratio per stage. The more that is understood about the flow properties leading to stall the better these technologies can be used to alter the flow in a way that inhibits stall cell formation. A two stage, high-speed, low aspect ratio fan was tested with three different casing treatments. Experimental data were obtained on the stage pressure characteristic shape, pressure ratio profile, high-response static pressures, and modal analysis at stall inception. From the analysis of this data the following conclusions about stall inception in this high-speed transonic fan can be made:

1) The different casing treatments did have an effect on the shape of the pressure characteristic at the near-stall operating condition. The results of this test show that flow conditions favoring stall inception may occur on the positive, neutral, or negative sloped portion of the stage pressure characteristic.

2) The near-stall pressure ratio profiles for the smooth case and circumferential grooves were similar in magnitude and shape at 68%, 85%, and 98.6% design corrected speed. At 68% and 85% speed the recirculating cavity was nearly evenly loaded from hub to tip corresponding to a higher pressure ratio and increased stall margin. At 98.6% speed the blockage induced by the recirculating flow was so significant as to reduce the total flow the rotor was able to pass.

3) Analysis of the high-response static pressure measurements show that fully developed rotating stall grew from a stall inception cell. For all stalls but 98.6% speed, smooth case, the frequency of the stall inception cell was 11% to 22% faster than fully developed rotating stall.

4) The casing treatments had a significant effect on the rotor tip flow which in turn influenced the stall inception characteristics of the fan. Each casing treatment and speed combination had a unique stall inception path. Variations in rotor tip flow effected the stall inception duration, stall inception cell frequency, existence of modal waves, duration of modal waves, and modal wave frequency.

5) Modal waves were detected for the circumferential groove and recirculating cavity casing treatments but not for smooth case. When modal waves were observed, they were found from 6 to 34 rotor revolutions prior to stall inception. Analysis of SFT phase data supports two different relationships between modal waves and stall inception. When modal waves and the stall inception cell are of the same frequency, the stall inception cell likely grows out of the modal wave. When modal waves are at a lower frequency than the stall inception cell, the modal waves are not strongly related to the stall inception cell.

ACKNOWLEDGEMENTS

The authors would like to acknowledge General Electric Aircraft Engine Company for the design of the fan. The data for this experiment was acquired as part of a test program which involved many individuals. The authors acknowledge the Technicians, Engineers, and Management of the Compressor Research Facility for the build-up, instrumentation, and test of the fan. In particular the authors would like to recognize Mark Burns of Battelle Memorial Institute for his help with the signal processing and data reduction, and Dr. Bill Copenhaver and Steve Puterbaugh of Wright Laboratory for their thought

provoking discussions and insights on casing treatments and stall inception in transonic fans.

REFERENCES

Boyer, K. M., King, P. I., and Copenhaver, W. W., 1993, "Stall Inception in Single Stage, High-Speed Compressors with Straight and Swept Leading Edges," AIAA paper 93-1870.

Day, I. J., 1993a, "Active Suppression of Rotating Stall and Surge in Axial Flow Compressors," ASME Journal of Turbomachinery, Vol. 115, pp. 40-47.

Day, I. J., 1993b, "Stall Inception in Axial Flow Compressors," ASME Journal of Turbomachinery, Vol. 115, pp. 1-9.

Day, I. J., and Freeman, C., 1993, "The Unstable Behavior of Low and High Speed Compressors," ASME paper 93-GT-26.

Emmons, H. W., Pearson, C. F., and Grant, H. P., 1955, "Compressor Surge and Stall Propagation," Transactions of the ASME, Vol. 77, pp. 455-469.

Epstein, A. H., Ffowcs Williams, J. E., and Greitzer, E. M., 1986, "Active Suppression of Aerodynamic Instabilities in Turbomachines," ASME Journal of Propulsion and Power, Vol. 5, No. 2, pp. 204-211.

Garnier, V. H., Epstein, A. H., and Greitzer, E. M., 1991, "Rotating Waves as a Stall Inception Indication in Axial Compressors," ASME Journal of Turbomachinery, Vol. 113, No. 2, pp. 290-302.

Greitzer, E. M., Nikkanen J. P., and Haddad, D. E., 1979, "A Fundamental Criterion for the Application of Rotor Casing Treatment," ASME Journal of Fluids Engineering, Vol. 101, pp. 237-244.

Hoying, D. H., 1993, "Stall Inception in a Multistage High Speed Axial Compressor," AIAA paper 93-2386.

McDougall, N. M., Cumpsty, N. A., and Hynes, T. P., 1990, "Stall Inception in Axial Compressors," ASME Journal of Turbomachinery, Vol. 112, pp. 116-125.

Moore, F. K., and Greitzer, E. M., 1986, "A Theory of Post-Stall Transients in Axial Compression Systems: Part I - Development of Equations, and Part II - Application," ASME Journal of Engineering for Gas Turbines and Power, Vol. 108, pp. 68-76 and 231-239.

Ostdiek, F. R., Copenhaver, W. W., and Rabe, D. C., 1989, "Compressor Performance Tests in the Compressor Research Facility." AGARD Conference on Unsteady Aerodynamic Phenomena in Turbomachines, Proceedings No. 468.

Paduano, J. D., Epstein, A. H., Valavani, L., Longley, J. P., Greitzer, E. M., and Guenette, G. R., 1991, "Active Control of Rotating Stall in a Low Speed Axial Compressor," ASME paper 91-GT-88.

Prince, Jr., D. C., Wisler, D. C., and Hilvers, D. E., 1975, "A Study of Casing Treatment Stall Margin Improvement Phenomena," ASME paper 75-GT-60.

Smith, G. D. J., and Cumpsty, N. A., 1984, "Flow Phenomena in Compressor Casing Treatment," ASME Journal of Engineering for Gas Turbines and Power, Vol. 106, pp. 532-541.

Stearns, S. D., and David, R. A., 1993, Signal Processing Algorithms in FORTRAN and C, Prentice-Hall, Inc., Englewood Cliffs, NJ, pp. 122-161.

Takata, H. and Tsukuda, Y., 1975 "Stall Margin Improvement by Casing Treatment - its Mechanism and Effectiveness," ASME paper 75-GT-13.

Tryfonidis, M., Etchevers, O., Paduano, J. D., Epstein, A. H., 1994, "Pre-Stall Behavior of Several High-Speed Compressors," Paper to be presented at the 1994 ASME IGTI Conference at The Hague, Netherlands.